Journal of proteome research

pubs.acs.org/jpr

Article

Metabolomics Meets Clinics: A Multivariate Analysis of Plasma and Urine Metabolic Signatures in Pulmonary Arterial Hypertension

Renata Wawrzyniak,* Peter Grešner, Ewa Lewicka, Szymon Macioszek, Artur Furga, Bożena Zieba, Michał J. Markuszewski, and Alicja Dąbrowska-Kugacka

Cite This: *J. Proteome Res.* 2024, 23, 2795−2804

Read Online

ACCESS | Metrics & More | Article Recommendations | Supporting Information

ABSTRACT: Pulmonary arterial hypertension (PAH) is a severe, multifactorial, and frequently misdiagnosed disorder. The aim of this observational study was to compare the plasma and urine metabolomic profiles of PAH patients and healthy control subjects. Plasma and urine metabolomic profiles were analyzed using the GC-MS technique. Correlations between metabolite levels and clinical parameters among PAH patients, as well as the between-group differences, were evaluated. The linear discriminant analysis model, which allows for subject classification in terms of PAH with the highest possible precision, was developed and proposed. Plasma pyruvic acid, cholesterol, threonine, urine 3-(3-hydroxyphenyl)-3-hydroxypropanoic acid, butyric acid, 1,2-benzenediol, glucoheptonic acid, and 2-oxo-glutaric acid were found to build a relatively accurate classification model for PAH patients. The model reached an accuracy of 91% and significantly improved subject classification (OR = 119 [95% CI: 20.3−698.3], $p < 0.0001$). Five metabolites were detected in urine that provide easily available and noninvasive tests as compared to right heart catheterization. The selected panel of metabolites has potential for early recognition of patients with dyspnea and faster referral to a reference center.

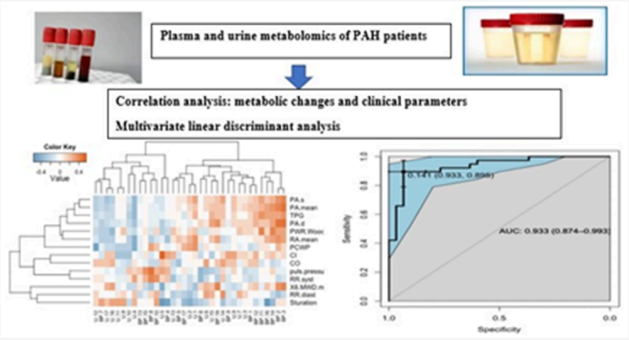

KEYWORDS: *metabolomics, pulmonary arterial hypertension, plasma, urine, multivariate analysis*

1. INTRODUCTION

Pulmonary hypertension (PH) constitutes a severe, multifactorial, and frequently misdiagnosed disorder.[1] PH is defined as a mean pulmonary arterial pressure (mPAP) above 20 mmHg at rest based on the Sixth World Symposium on Pulmonary Hypertension[2] as well as above 25 mmHg at rest based on the European Society of Cardiology (ESC)/European Respiratory Society (ERS) guidelines.[3] However, from the clinical perspective, additional parameters such as pulmonary vascular resistance (PVR) and pulmonary capillary wedge pressure (PCWP) provide a more useful hemodynamic signature of the disease. According to WHO, ESC 2016, and the Sixth World Symposium on Pulmonary Hypertension guidelines, PH is categorized into five groups.[2,3] This classification is based on clinical symptoms, pathological hallmarks, hemodynamic parameters, and treatment strategy.

Pulmonary arterial hypertension (PAH) constitutes a term that specifically indicates WHO group 1. There are a few subtypes of PAH related to various etiologies (i.e., idiopathic, heritable, drug, and toxin induced), different disorders (i.e., connective tissue disease, congenital heart disease, portal hypertension, human immunodeficiency virus infection, and schistosomiasis), and features of pulmonary veno-occlusive disease/or pulmonary capillary hemangiomatosis. The main histopathological modification in PAH patients includes remodeling of the pulmonary vasculature as a result of abnormal proliferation of the smooth muscle cells lining the pulmonary arteries, which leads to increased PVR.[4] Misdiagnosed or unrecognized PAH can lead to right ventricular dysfunction and, consequently, eventual premature death. The pathophysiological processes accompanying PAH have not yet been fully elucidated. Basic knowledge about the potential pathomechanisms of the disease is mainly based on experimental animal models.[5−7] The diagnostic process of PAH is complex, as other causes of PH have to be excluded, and no specific marker of the arterial etiology of PH has been identified. Invasive right heart catheterization (RHC) remains the gold standard of proper diagnosis and the key guidance of PAH treatment. Therefore, there is still an urgent need to explore and propose noninvasive and more specific diagnostic indicators of the disease.[8]

Special Issue: Women in Proteomics and Metabolomics

Received: May 3, 2023
Published: October 12, 2023

https://doi.org/10.1021/acs.jproteome.3c00255
J. Proteome Res. 2024, 23, 2795−2804

Table 1. Baseline Clinical Characteristics of Patients with the Pulmonary Arterial Hypertension Group (n = 43)[a]

variables			
age (years)	46 ± 18		
females (n/%)	27 (64%)		
height (cm)	162 ± 10		
weight (kg)	67 ± 15		
BMI (kg/m^2)	26 ± 6		
PAH classification (n/%)			
idiopathic	22 (51%)		
connective tissue disease	3 (7%)		
congenital heart disease	18 (42%)		
WHO functional class (n/%)			
I	1 (2%)		
II	18 (42%)		
III	16 (37%)		
IV	8 (19%)		
comorbidities (n/%)			
arterial hypertension	10 (23%)		
hypothyreosis	12 (28%)		
diabetes mellitus	5 (12%)		
renal failure	4 (9%)		
coronary artery disease	6 (14%)		
lung disease	8 (19%)		
paroxysmal/persistent AF	2 (5%)		
physiological measurements	LQ	median	UQ
HR (beats/min)	68.50	77.0	85.50
SBP (mmHg)	101.75	115.50	125.75
DBP (mmHg)	65.25	70.00	77.00
pulse pressure (mmHg)	34.00	41.50	52.50
laboratory measurements	LQ	median	UQ
BNP (pg/mL)	22.0	51.0	110.00
hemoglobin (g/dL)	13.33	16.20	19.17
PLT (thou./uL)	153.00	187.50	226.50
sodium (mmol/L)	136.25	138.00	140.00
iron (μg/dL)	55.00	79.00	103.00
uric acid (mg/dL)	5.40	6.40	7.80
bilirubin (mg/dL)	0.60	1.08	1.44
GGT (U/L)	16.0	29.00	56.50
ALP (U/L)	59.0	72.0	89.0
AST (U/L)	15.0	19.0	24.0
ALT (U/L)	13.0	18.0	25.0
creatinine (mg/dL)	0.72	0.85	1.09
6MWT (m)	329.50	399.0	500.50
PAH-specific treatment (n/%)			
calcium blockers	4 (9%)		
bosentan	14 (33%)		
macitentan	4 (9%)		
sildenafil	27 (63%)		
inhaled iloprost	6 (14%)		
treprostinil s.c.	11 (26%)		
combined therapy	22 (51%)		
other medication (n/%)			
beta blockers	4 (9%)		
statins	9 (21%)		
ACEI/sartans	6 (14%)		
diuretics	17 (40%)		
anticoagulants	8 (19%)		
euthyrox	10 (23%)		
other	22 (51%)		
right heart catheterization parameters	LQ	median	UQ
mPAP (mmHg)	46.0	56.0	71.0
PCWP (mmHg)	6.25	9.0	11.0
mRAP (mmHg)	3.75	5.50	8.0
CI (mL/kg/min)	1.99	2.60	3.05
PVR (Wood units)	6.55	10.84	15.55
echocardiographic variables	LQ	median	UQ
RVEDD (mm)	37.0	44.0	49.50
LVEDD (mm)	32.0	38.0	42.0
RV:LV	1.0	1.10	1.35
right atrial area (cm^2)	14.80	19.60	24.85
tricuspid regurgitant velocity (m/s)	3.50	4.14	4.42
RVSP (mmHg)	56.0	79.0	90.0
TAPSE (mm)	16.50	19.0	22.0
RV S′ (cm/s)	10.0	12.0	14.0
RVFAC (%)	0.29	0.34	0.43
RVstrain (%)	−23.75	−19.50	−14.0
LVEF (%)	54.0	59.0	64.0
LVESV (mL)	21.0	30.0	35.50
LVEDV (mL)	54.0	68.0	84.0
LV GLS (%)	−21.0	−19.0	−16.0
pericardial effusion (number of pts/%)	6 (14%)		

[a]WHO−World Health Organization, AF−atrial fibrillation, HR−heart rate, SBP−systolic blood pressure, DBP−diastolic blood pressure, BNP−brain natriuretic peptide, PLT−platelet count, GGT−gamma-glutamyltranspeptidase, ALP−alkaline phosphatase, AST−aspartate aminotransferase, ALT−alanine aminotransferase, 6MWT−6 min walk test, s.c.−subcutaneous, ACEI−angiotensin-converting enzyme inhibitor, ARB−angiotensin receptor blocker, mPA−mean pulmonary artery pressure, PCWP−pulmonary capillary wedge pressure, mRAP−mean right atrial pressure, CI−cardiac index, PVR−pulmonary vascular resistance, RVEDD−right ventricular (RV) end-diastolic diameter in apical 4-chamber view, LVESD−left ventricular (LV) end-systolic diameter in apical 4-chamber view, RV:LV−the ratio of RVEDD to LVEDD, RVSP−RV systolic pressure, TAPSE−tricuspid annular plane systolic excursion, S′−tissue Doppler-derived tricuspid lateral annular systolic velocity, RVFAC−RV fractional area change, LVEF−left ventricular ejection fraction, LV GLS−left ventricular global longitudinal strain in 2-dimensional speckle trackingstrain analysis; n−number of patients, data presented as mean ± standard deviation or as median and lower quartile (LQ) as well as upper quartile (UQ).

Metabolomics offers a promising approach to evaluate comprehensive metabolic signatures of both physiological and pathophysiological states in biological systems. As a part of omics sciences, metabolomics constitutes the end point of genome alterations and provides better representation of the phenotype compared to gene or protein expression levels.[9] Measured metabolite levels reflect the integrated variation derived from genomic, transcriptomic, proteomic, epigenetic, and environmental factors. Therefore, untargeted metabolomics, which aims to detect as many metabolites in biological samples as possible, can provide useful and comprehensive knowledge about altered biochemical pathways in PAH. So far, some applications of untargeted metabolomics in PAH patients have been reported.[10−15] However, only one type of biological material has been evaluated in terms of metabolic alterations. These recent reports concern mainly serum, plasma, exhaled breath condensate, or lung tissue samples. In our study both plasma and urine metabolomic profiles of PAH patients were

https://doi.org/10.1021/acs.jproteome.3c00255
J. Proteome Res. 2024, 23, 2795−2804

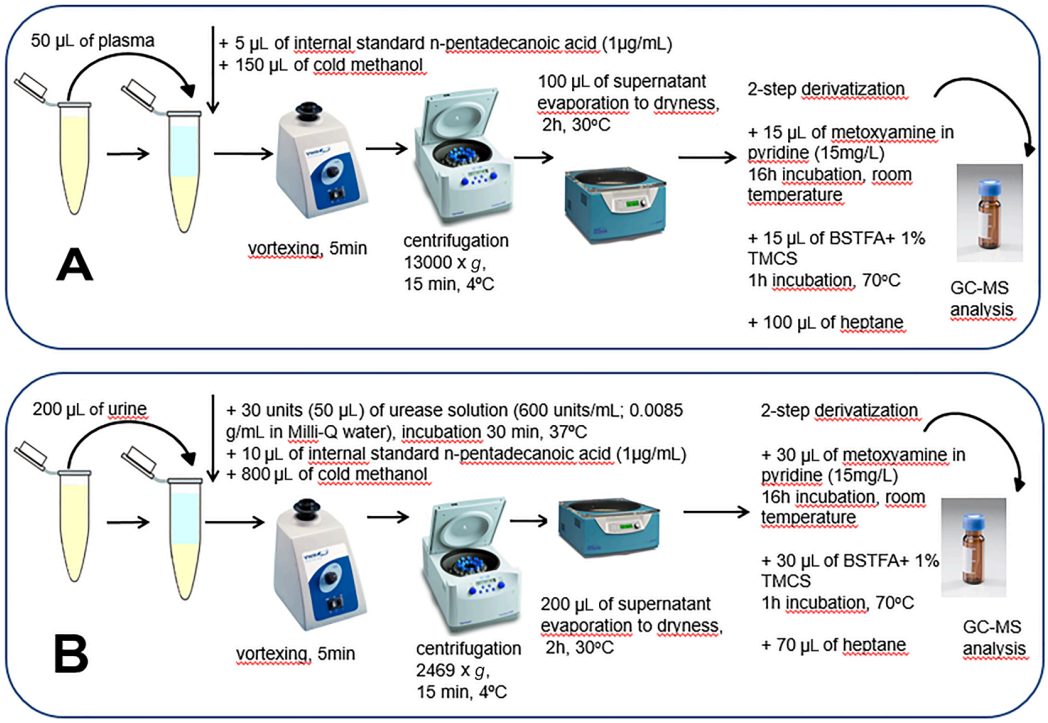

Figure 1. Plasma (A) and urine (B) preparation procedures for untargeted metabolomic analyses.

compared with a control group. Additionally, the observed metabolic changes have rarely been correlated with clinical parameters from RHC to provide more specific metabolic indicators of PAH.

Therefore, the aim of this observational study was to analyze the plasma and urine metabolomic profiles of PAH patients and healthy control subjects. We searched for correlations between metabolite levels and clinical parameters among PAH patients, as well as between-group differences in selected plasma/urine metabolite levels. Furthermore, we proposed a multivariate classification model based on measured metabolomic parameters, allowing for subject classification in terms of PAH with the highest possible precision. The model's performance has also been thoroughly characterized.

2. MATERIALS AND METHODS

2.1. The Study Groups

This was an observational study that included 43 adult PAH patients treated according to the Polish Health Fund program in the Department of Cardiology Medical University of Gdańsk. This program was introduced in Poland in 2009 and included patients with a definite diagnosis of PAH and RV failure of at least WHO Class III. The diagnosis of PAH was established by RHC in the presence of an increase in mean pulmonary arterial pressure ≥25 mmHg at rest and pulmonary artery wedge pressure ≤15 mmHg in the absence of other causes of precapillary pulmonary hypertension. Thus, patients with pulmonary hypertension due to left heart disease, lung disease, thromboembolic, or other rare disorders were excluded. The date of PAH diagnosis corresponded to the date of confirmatory RHC. Patients with Eisenmenger syndrome and a confirmatory RHC in childhood did not need to have the RHC repeated before implementation of the PAH-specific treatment. Routine evaluation, performed every 6 months, included PAH medical history and comorbidities, assessment of the WHO functional class, physical examination, electrocardiography (ECG), echocardiography, blood sample analysis, and nonencouraged 6 min walk test (6MWT), performed according to American Thoracic Society recommendations. The baseline demographic and clinical characteristics of PAH patients enrolled in this study are provided in Table 1.

The control group (n = 37) consisted of age (p = 0.506), sex (p = 0.193), and body-surface-area (p = 0.114) matched healthy volunteers drawn from a general population. The study was conducted in accordance with the Declaration of Helsinki and was granted approval by the Ethical Committee of the Medical University of Gdańsk (number of approval: NKBBN/204/2018). All participants included in this study signed their informed consent forms.

2.2. Plasma and Urine Collection

Plasma and urine samples were collected from all PAH patients and controls. First morning urine samples (10 mL) were obtained as midstream urine specimens after perineal cleansing. Fasting peripheral vein blood samples were collected with 5 mL lithium heparin tubes. Urine samples were centrifuged before storage (10 min, 2000g, at 4 °C). The whole blood samples were centrifuged (10 min, 2000g, 4 °C) to obtain plasma fractions. Collected urine and plasma samples were stored at −80 °C until metabolomics experiments. Directly before analysis, the urine and plasma samples were thawed at room temperature or in ice, respectively.

2.3. Metabolomic Analyses Using the GC-MS Technique

Plasma and urine samples were prepared according to previously published procedures.[16,17] Briefly, urine samples, after removing the redundant amount of urea, were diluted with cold methanol, evaporated to dryness, and derivatized with the use of a two-step procedure before analytical

https://doi.org/10.1021/acs.jproteome.3c00255
J. Proteome Res. 2024, 23, 2795−2804

measurements. Plasma samples were deproteinized with cold methanol, evaporated to dryness, and underwent the same two-step derivatization procedure before metabolomics analyses. Detailed sample preparation procedures are presented in Figure 1. Additionally, pooled biological samples prepared by mixing the 50 μL aliquots of each plasma or urine sample were used as the quality control samples (QC) to monitor the system stability and method reproducibility during all sequence runs. QCs were prepared according to the same procedures as plasma and urine samples.

Plasma and urine metabolomic profiles were obtained with the use of the GC-MS technique.[16] Analytical measurements were performed using GCMS-TQ8030 (Shimadzu, Japan) equipped with an electron ionization source (EI). Here, 1 μL of each urine and plasma sample was injected in a splitless mode into a Zebron ZB-5MS column (30 m × 0.25 mm, 0.25 μm, Phenomenex, USA). Details on parameters of the previously optimized analytical method are described in the Supporting Information (Figure S1).

The obtained raw data were processed (peak detection, deconvolution, alignment, and compound identification) with the use of Automated Mass Spectral Deconvolution and Identification Software (AMDIS) with the NIST11 spectra library (www.amdis.net) and in-house spectra library based on the Wiley 10th library. Detected compounds were annotated based on retention time (RT), retention index (RI), and mass spectrum. Subsequently, data filtration was conducted using MassProfiler Professional B.02.02 software (Agilent Technologies, Waldbronn, Germany). Data filtration was based on compound frequency (presence in at least 80% of samples in one out of two groups: PAH or control) and quality assurance criteria (presence in at least 50% of all QCs and coefficient of variation in peak intensity lower than 30%).[18] The data matrices obtained were normalized with the use of probabilistic quotient normalization (PQN) prior to univariate and multivariate statistical analyses.

2.4. Statistical Analysis

First, the reproducibility of analytical measurements was verified by unsupervised principal component analysis (PCA). Afterward, orthogonal partial least-squares discriminant analysis (OPLS-DA) was used to select plasma and urine metabolites, allowing the best discrimination between the control and PAH groups.

The normality of both metabolomic and clinical data distributions was checked using the Shapiro−Wilk W test. Simple correlations between metabolomic and clinical parameters in the PAH group were sought for by means of Spearman's rank correlation method, and the strength of correlations was expressed by means of Spearman's correlation coefficient r_{SP}. Additionally, the proportion of overall variability of the experimental data explained by the correlation was expressed by the coefficient of determination R^2. Results of correlation analysis were then subject to unsupervised clustering (using the Ward's method) in order to identify clusters of parameters with similar correlational behavior, which were presented in the form of a correlation matrix (i.e., heatmap). For the sake of increased readability, the heatmap shows only statistically and marginally significant ($p < 0.06$) correlations. Simple differences between the control and PAH groups in plasma and urine metabolic parameters were tested for statistical significance using the Mann−Whitney U test, as many of the analyzed plasma and urine metabolic parameters presented non-Gaussian distribution.

In the subsequent stage of statistical analysis, multivariate modeling based on the linear discriminant analysis (LDA) method was performed to obtain a classification model capable of patient classification (control/PAH) based on measured plasma and urine metabolite levels. The dimensionality of the data set used in LDA modeling was further reduced by means of yet another PCA step, the outcomes of which, combined with those obtained from simple one-dimensional between-group comparisons, were used to preselect the variables involved further in the modeling. Hence, only metabolites with statistically significant between-group differences ($p < 0.1$), which, at the same time, were identified among the top contributors (four metabolites with the highest positive and the lowest negative variable loadings) to the first four PCA components (the number of components was chosen arbitrarily), were subsequently involved in the modeling. Following this preselection step, an exhaustive examination of all possible models from the second to the highest possible order of dimensionality was performed. All examined models were trained on a training set (70% of the initial data set) and described by classification error, that is, the percentage of incorrectly classified observations of the test set (30% of the initial set). To increase the robustness of the examined LDA models against the nonrandom split bias, random selection of observations for the training and the test set, as well as the classification error determination, was repeated 50 times, and each model was then characterized by the mean classification error. The model with the lowest mean classification error was then picked as the best classification model and further analyzed by the receiver operating characteristic (ROC) curve analysis to determine the best threshold value (Thres), ensuring the highest possible model performance. Model characteristics derived from the obtained ROC curve that accurately describe the model performance given the determined threshold value include the following: area under the curve (AUC), sensitivity (Sens), specificity (Spec), accuracy (Acc), and odds ratio (OR).

3. RESULTS

3.1. Initial Analysis of Metabolomic Signatures of the Study Groups

Exemplary plasma and urine metabolomic profiles measured with the use of the GC-MS technique are presented in Figure S1. Raw data processing and filtration resulted in 65 and 77 plasma and urine metabolites, respectively, which were then normalized prior to further statistical analysis and subject to verification of reproducibility of analytical measurements by PCA. Two-dimensional representations of all analyzed samples based on the obtained PCA model for both plasma and urine samples are presented in Figures S2 and S3 (panels A) in the Supporting Information. In contrast to samples from PAH patients and controls, the QC samples presented a relatively high degree of clustering in PCA model-based representations, which indicates the GC-MS system's stability, the reproducibility of the sample preparation procedures, and analytical measurements, thus allowing us to assume that any metabolic changes observed in PAH patients compared to controls were mainly due to biological rather than analytical variation.

Based on the results of subsequent OPLS-DA modeling, the initially selected panel of 65 and 77 metabolites was further

https://doi.org/10.1021/acs.jproteome.3c00255
J. Proteome Res. 2024, 23, 2795−2804

reduced to 18 plasma and 17 urine metabolites, which were then involved in further statistical analyses (Figures S2 and S3, panels B and Table 2). The panels of plasma and urine

Table 2. Panel of Both Blood Plasma and Urine Metabolites Selected for Statistical Analysis

metabolite	symbol[a]
pyruvic acid	BP.1
leucine	BP.2
valine	BP.3
ribose	BP.4
lysine	BP.5
phosphoric acid	BP.6
sucrose	BP.7
3,4-dihydroxybutanoic acid	BP.8
lactic acid	BP.9
sorbitol	BP.10
fructose	BP.11
nonanic acid	BP.12
maltose	BP.13
octadecanoic acid	BP.14
inositol	BP.15
cholesterol	BP.16
3-butanoic acid	BP.17
threonine	BP.18
hippuric acid	U.1
3(-3-hydroxyphenyl)-3-hydroxypropanoic acid	U.2
tagatose	U.3
butyric acid	U.4
1,2-benzenediol	U.5
butanoic acid	U.6
glucoheptonic acid	U.7
2,3-dihydroxybutanoic acid	U.8
acetic acid	U.9
2-oxo-glutaric acid	U.10
threonic acid	U.11
mannonic acid	U.12
ribonic acid	U.13
2-methyl-3-oxopropanoic acid	U.14
2-propenoic acid	U.15
stearic acid	U.16
lactose	U.17

[a]BP = blood plasma and U = urine.

metabolites were selected by OPLS-DA based on VIP (>1.0) and |p(corr))| (>0.4) criteria. Most of these metabolites showed non-Gaussian distribution in both groups; therefore, their distributions were described by means of nonparametric measures (median and interquartile range (IQR); Table S1). In the case of clinical data (PAH subjects only), most of the data (except for PCWP and PWR) showed normal distribution. The mean and standard deviation (SD) were thus used to describe the data distribution (Table S2).

3.2. between-Group Differences in Plasma and Urine Metabolomic Profiles

Univariate analyses of simple between-group differences between PAH patients and control subjects revealed that PAH patients presented significantly higher median plasma concentrations of ribose ($p < 0.05$), sucrose ($p < 0.005$), 3,4-dihydroxybutanoic acid ($p < 0.0005$), and cholesterol ($p < 0.01$) but significantly lower median plasma concentrations of pyruvic acid ($p < 0.005$), leucine ($p < 0.001$), valine ($p < 0.005$), lysine ($p < 0.05$), lactic acid ($p < 0.0005$), and threonine ($p \ll 0.0001$) as compared to controls.

In the case of urine samples, PAH patients were found to show significantly higher median urine concentrations of butyric acid ($p < 0.0005$), glucoheptonic acid ($p = 0.005$), 2-pentanedioic acid ($p < 0.0001$), threonic acid ($p < 0.05$), and ribonic acid ($p < 0.05$) but significantly lower median concentrations of hippuric acid ($p < 0.05$), 3-hydroxypropionic acid ($p < 0.01$), tagatose ($p < 0.005$), 1,2-benezediol ($p < 0.01$), butanoic acid ($p < 0.005$), and acetic acid ($p < 0.05$) compared to controls. Graphical presentation of between-group differences in plasma and urine metabolite concentrations are included in the Supporting Information (Figures S4−S5).

3.3. Correlation Analysis of Plasma and Urine Metabolites in PAH Patients

In simple correlation analyses, the metabolomic data (from both blood plasma and urine) of PAH patients were correlated with their clinical parameters. Figure 2 shows a correlation matrix between clinical and metabolomic parameters in the form of a heat map following the employment of unsupervised hierarchical clustering. One can easily distinguish a cluster of seven clinical parameters (PA.s, PA.mean, TPG, PA.d, PWR.Wood, RA.mean, and PCWP) that seem to present moderate or relatively strong positive correlation with fructose, cholesterol, stearic acid, leucine, and valine, while presenting moderate or relatively strong negative correlation with mannonic acid, sucrose, lactose, stearic acid, 2-oxo-glutaric acid, and butyric acid. Full details on these correlations can be found in a thorough summary of the correlation analyses in the Supporting Information (Table S3). The most significant correlations between clinical and metabolomic parameters were selected based on $p < 0.05$ and $|r_{SP}| > 0.333$ criteria. However, correlations for only the most prognostic clinical parameters are presented in Table 3.

3.4. Data Dimensionality Reduction

To further reduce the dimensionality of metabolomics data, the panel of 18 plasma and 17 urine metabolites selected via initial OPLS-DA modeling was further submitted to PCA, the results of which were combined with the outcomes of the above-described univariate analyses of simple between-group differences (for details, see Materials and Methods). The obtained outcomes suggest that the first four principal components explain 39% of the initial variability of the data set. Basic characteristics of these components, including SD, variability, and the absolute and cumulative fractions of variability of the initial data set explained by individual components, can be found in the Supporting Information (Table S4), while the structure of individual components is presented in Table S5.

The first principal component (PC1), explaining 15% of the data variability, was positively correlated with urine 2-pentanedioic acid, threonic acid, and butyric acid as well as plasma ribose levels. It was also negatively correlated with urine butanoic acid as well as plasma stearic acid, valine, and leucine levels (see Table S5). Furthermore, we found significantly higher values of PC1 in the PAH group compared to controls ($p < 0.0001$; Figure S5), which implies that PAH patients, contrary to controls, can in general be expected to show higher urine levels of 2-pentanedioic, threonic, and butyric acids together with higher plasma ribose levels, as well as lower urine levels of butanoic acid together with lower

https://doi.org/10.1021/acs.jproteome.3c00255
J. Proteome Res. 2024, 23, 2795−2804

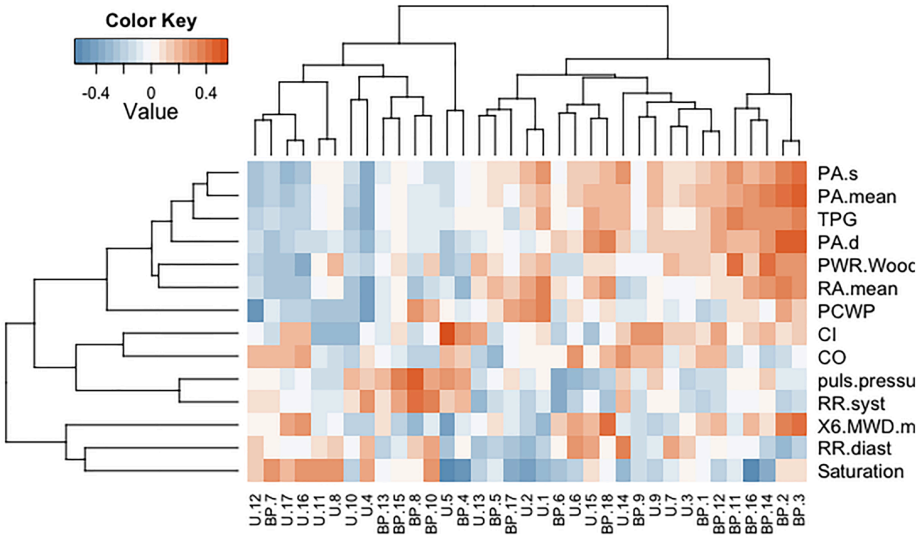

Figure 2. Correlation matrix showing the results of correlation analyses among metabolic and clinical parameters in the PAH group. Presented are the values of the Spearman's regression coefficients (r_{SP}), whereas the full details (including the respective levels of significance) can be found in the Supporting Information, Table S3. The unsupervised hierarchical clustering was conducted using Ward's method.

Table 3. List of the Most Interesting Statistically Significant Correlations between Metabolomic and Clinical Parameters in the PAH Group Found in the Study[a]

correlation	r_{SP}	R^2	p
6MDW (m) and threonine (BP18)	0.412	0.169	0.014
RR.syst. and 3,4-dihydroxybutanoic acid (BP8)	0.427	0.182	0.008
RR.diast and 2-methyl-3-oxopropanoic acid (U14)	0.334	0.112	0.043
saturation and cholesterol (BP16)	−0.555	0.309	0.014
pulse pressure and 3,4-dihydroxybutanoic acid (BP8)	0.460	0.212	0.004
PA.s and valine (BP3)	0.405	0.164	0.018
PA.s and butyric acid (U4)	−0.352	0.124	0.041
PA.d and valine (BP3)	0.483	0.233	0.004
PA.mean and valine (BP3)	0.455	0.207	0.007
PA.mean and stearic acid (BP14)	0.344	0.118	0.046
PA.mean and butyric acid (U4)	−0.356	0.126	0.039
PCWP and butyric acid (U4)	−0.400	0.160	0.029
RA.mean and butyric acid (U4)	−0.426	0.181	0.017
CI and 1,2-benzenediol (U5)	0.544	0.296	0.032
PVR and stearic acid (BP14)	0.411	0.169	0.016
PVR and stearic acid (U16)	−0.348	0.121	0.044

[a]6MDW (m): 6 min walking distance, RR.syst. (mmHg): systolic blood pressure, RR.diast. (mmHg): diastolic blood pressure, PA.s (mmHg): systolic pulmonary artery pressure, PA.d (mmHg): diastolic pulmonary artery pressure, PA.mean (mmHg): mean pulmonary artery pressure, PCWP (mmHg): pulmonary capillary wedge pressure, RA.mean (mmHg): mean right atrial pressure, CI (mL/kg/min): cardiac index, PVR (Wood): pulmonary vascular resistance. Full results of correlation analyses can be found in the Supporting Information file (Table S1). r_{SP}—Spearman's correlation coefficient; R^2—coefficient of determination; p-level of significance.

plasma levels of stearic acid, valine, and leucine. The remaining principal components did not show any statistically significant differences between the groups (Figure S6).

Employing the data dimensionality reduction approach resulted in reducing the panel of 35 metabolites to only 16, which were further involved in building the LDA model (Table S6).

3.5. Linear Discriminant Analysis

In multivariate LDA-based modeling, only 16 previously selected metabolites were involved. An exhaustive examination of all possible models of the second to 16th order of dimensionality was performed. In all, we thus examined 65 519 various models. The best LDA model was selected based on the lowest mean classification error in a test set, which was found to be 0.164 in the case of an eighth-order model consisting of three plasma (pyruvic acid (BP.1), cholesterol (BP.16), and threonine (BP.18)) and five urine (3-(3-hydroxyphenyl)-3-hydroxypropanoic acid (U.2), butyric acid (U.4), 1,2-benzenediol (U.5), glucoheptonic acid (U.7), and 2-oxo-glutaric acid (U.10)) metabolites (Table 4). A summary of mean classification errors in a test set of all examined models can be found in the Supporting Information (Figure S7).

The model reached a high level of statistical significance ($p < 0.0001$), and the ROC analysis confirmed its relatively good overall performance (see Figure 3). The area under the ROC curve of the model was 0.93 (95% CI: 0.87−0.99), model sensitivity was 0.89 (95% CI: 0.79−0.97), and its specificity

Table 4. Characteristics of the LDA Model with the Lowest Mean Classification Error[a]

symbol	metabolite	Raw	Struct
BP1	pyruvic acid	2.2300	0.5882
BP16	cholesterol	−0.6498	−0.1867
BP18	threonine	0.2466	−0.0040
U2	3-(3-hydroxyphenyl)-3-hydroxypropanoic acid	0.4898	0.4943
U4	butyric acid	1.0486	0.5213
U5	1,2-benzenediol	1.0785	0.4223
U7	glucoheptonic acid	−1.9540	−0.4782
U10	2-oxo-glutaric acid	−0.9902	−0.5636

[a]The table shows the structure of the best LDA model found in the study with raw (Raw) and structure (Struc) coefficients for individual variables in the model.

https://doi.org/10.1021/acs.jproteome.3c00255
J. Proteome Res. 2024, 23, 2795−2804

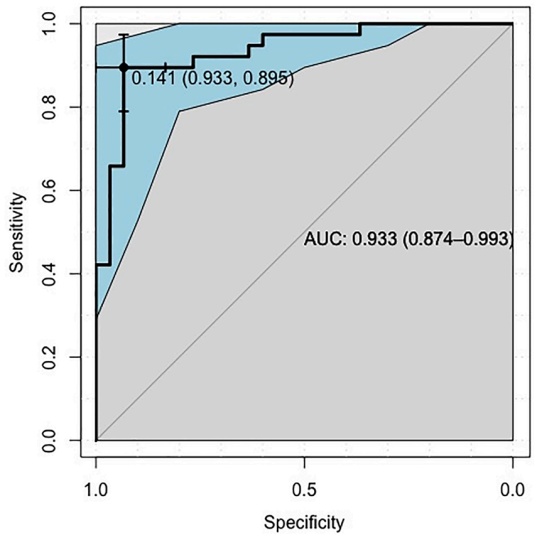

Figure 3. ROC curve with 95% confidence interval (blue field) summarizing the performance of the best LDA model in a training set of subjects. The value of 0.141 was revealed as the best threshold for ensuring the best classification of subjects (AUC: 0.933 [0.874−0.993]; sensitivity: 0.89 [0.79−0.97]; specificity: 0.93 [0.83−1.00]; accuracy: 0.91; OR = 119 [20.3−698.3]).

was 0.93 (95% CI: 0.83−1.00). The model reached an accuracy of 91% and turned out to significantly improve subject classification (OR = 119 [95% CI: 20.3−698.3], $p < 0.0001$).

4. DISCUSSION

In this study, we searched for plasma and urine metabolites plausibly correlated with RHC parameters among PAH patients. The panel of metabolites that were found to be significantly correlated with clinical parameters included valine and stearic acid measured in plasma as well as 2-methylpropanoic, 1,2-benzenediol, and stearic acid detected in urine samples. Valine (2-amino-3-methyl-butanoic acid), as an amino acid, serves as a precursor for the synthesis of various molecules playing an essential role in homeostasis.[19] In a recent animal-based study, valine was observed to lower the level of plasma triglycerides, thus having a positive effect on lipid balance and, consequently, on the integrity of the vascular wall.[20] Similar to these results, Noguchi et al. highlighted the role of both valine and leucine in counteracting the impact of abnormal lipid content, which is directly involved in the production of atherosclerotic lesions.[21] In our study, plasma valine level was positively correlated with clinical parameters constituting specific and diagnostic markers of the disease, such as PA.s, PA.d, and PA.mean. Higher plasma levels of valine corresponded to higher PA.d and PA.mean values, which could be related to disease progression.

In our study, the plasma level of stearic acid was positively correlated with PA.mean and PVR, while the urine level of its metabolite was negatively correlated with PVR. These correlations are consistent with the progression of PAH. Stearic acid, also known as octadecanoic acid, is a saturated long-chain fatty acid with an 18-carbon backbone found in all living organisms. Following its biosynthesis, it may undergo a variety of reactions, including desaturation to oleate,[22] after which it then plays its role in the synthesis of triglycerides and other complex lipids. Recently, a potential role of stearic acid in idiopathic pulmonary fibrosis (IPF) has been suggested by a study reporting lower levels of stearic acid in IPF lung tissues as compared to controls.[23] Moreover, the same study provided evidence on the antifibrotic role of stearic acid in a bleomycin-induced lung fibrosis mouse model.[23] It was concluded that stearic acid may exert its antifibrotic activity by regulation of profibrotic signaling and by reduction of TGF-β1-induced α-SMA and collagen type 1 expression.[23] Whether or not such mechanisms may be relevant to PAH needs to be verified.

In our study, a significantly negative correlation between urine butyric acid and PA.s, PA.mean, PCWP, and RA.mean was observed in the PAH group. This correlation is consistent with the severity of PAH. Regarding PCWP, its higher value probably corresponds to disease progression, but the additional impact of LV dysfunction and venous circulation should be considered. Butyric acid is one of three common short-chain fatty acids (SCFAs) in the human gut.[24] In the colon, it serves various crucial roles, such as constituting a source of energy for endothelial cells, promoting cell differentiation and apoptosis, and inhibiting colonic acidification.[25] It is also involved in inhibition of breakdown of fats (via hydroxycarboxylic acid receptor 2), as well as in stabilization of lipid metabolism (via peroxisome proliferator-activated receptor), making it one of the key compounds in regulation of lipid metabolism. Butyric acid regulates inflammatory processes by stimulating the production of eicosanoids[26] and was shown to inhibit cancer cell proliferation in the colon.[27] In animal models, butyrate supplementation can reduce atherosclerotic lesions and affect arterial blood pleasure, showing a significant hypotensive effect when its concentration in the colon increases.[28] In general, SCFAs are known as signaling molecules between gut microbiota and host, with receptors in various cell and tissue types.[29] There is a well-established link between gut microbiota and coronary artery disease and atherosclerosis. The role of changes in the gut and circulating microbiome in the initiation of perivascular inflammation in the early pathogenesis of PAH has also been reviewed.[30]

In PAH subjects, we further found that urine 1,2-benzenediol levels were positively correlated with CI. This metabolite, also known as pyrocatechol (catechol), is formed endogenously in biological systems from neurotransmitters including adrenaline, noradrenaline, and dopamine, although it is also a metabolite of many drugs like DOPA, isoproterenol, and acetylsalicylic acid or a product of transformation of xenobiotics.[31] Catechol was found to provoke necrotic, apoptotic, and morphological changes, as well as increased lipid peroxidation and protein carbonylation in peripheral blood mononuclear cells, mainly lymphocytes.[32] Furthermore, the activity of catechol-*O*-methyltransferase (COMT), an enzyme responsible for inactivation of catecholamines, was recently studied in relation to regulation of blood pressure in humans.[33] It was suggested that multiple system atrophy constitutes an excellent model for evaluating the effect of subtle manipulations in norepinephrine metabolism on blood pressure regulation in small numbers of subjects.

In our study, we also focused on searching for eventual between-group differences in selected plasma and urine metabolites, which would plausibly allow us to build a classificator capable of proper subject classification into PAH and control group based on observed metabolomic profile. Elaborated on and presented was an eight-dimensional LDA model, based on plasma pyruvic acid, cholesterol, and threonine as well as urine 3-(3-hydroxyphenyl)-3-hydroxypro-

https://doi.org/10.1021/acs.jproteome.3c00255
J. Proteome Res. 2024, 23, 2795−2804

panoic acid, butyric acid, 1,2-benzenediol, glucoheptonic acid, and 2-oxoglutaric acid. In the context of PAH pathogenesis, especially pyruvic acid, 2-oxo-glutaric and cholesterol are relevant and should be marked. Metabolic changes in these substances are mainly related to alterations in glycolysis and glucose oxidation, fatty acid metabolism, and tricarboxylic acid (TCA) cycle.[34]

Glucose is metabolized to pyruvate through the glycolysis pathway. In PAH, glucose metabolism is shifted from oxidative phosphorylation toward glycolytic conversion to pyruvate and subsequently to lactate. Such metabolic signatures were observed in primary pulmonary artery endothelial cells (PAEC) and pulmonary artery smooth muscle cell lines (PASMC) derived from PAH lungs in the hearts and lungs of patients with PAH in vivo, as well as in PAH animal models.[14,35−38] The molecular mechanisms promoting the shift to glycolysis in PAH are mainly related to the excessive accumulation of hypoxia-inducible factor HIF-1. Upregulation of this transcription factor was previously observed in plexiform lesions, pulmonary arteries, and cardiomyocytes from PAH patients.[35,37,39,40] In this study, however, lower plasma levels of pyruvate and lactate were observed, which contradicts the above-described findings and requires further investigation. It should be mentioned that previous observations were derived mainly from pathologically altered tissue and cell samples. In this study, decreased plasma pyruvate and lactate levels reflect global metabolic response for PAH.

Furthermore, 2-oxoglutaric acid, also known as alpha-ketoglutaric acid (AKG), is a key molecule in the TCA cycle, playing a fundamental role in determining the overall rate of this metabolic pathway.[41] The upregulation of the TCA cycle was previously found in PAH lung tissue.[14] Most intermediates of the TCA cycle, including citrate and *cis*-aconitate, were significantly increased in lung tissue. Moreover, highly significant overexpression of the isocitrate dehydrogenase 1 gene (IDH1, coding an enzyme catalyzing the AKG production from isocitrate) in the lungs of PAH patients was observed. Our findings concerning the AKG levels in urine reported in this study corroborate well with the above-mentioned reports, which further strengthens the hypothesis that increased metabolites and related gene expression in the TCA cycle may reflect abnormalities in mitochondrial function in PAH patients.

In our study, we also observed increased blood plasma cholesterol levels in PAH patients. It is well-known that in blood plasma, cholesterol esters are transported as lipoprotein particles such as chylomicrons and low-density and high-density lipoproteins. Low-density lipoprotein cholesterol (LDL-C) is a well-established marker of cardiovascular risk,[42] but its association with PAH patients' survival has also been observed.[43] It was observed that LDL-C levels were low in patients with PAH and were related to an increased risk of death. Moreover, LDL-C levels appeared not to respond to PH reversal, as they were found to be lower in both PAH and chronic thromboembolic pulmonary hypertension (CTEPH) patients undergoing invasive treatment as compared to controls.[43] HDL-C has recently also been reported to be associated with PAH patients' prognoses.[44] This effect is believed to be mediated by its vasoprotective activity, the main role which is played by the vascular endothelium, also a crucial player in PAH pathobiology. The potential vasoprotective mechanisms of HDL in pulmonary circulation have been reviewed.[45] In our study, we measured the plasma total levels of cholesterol, which were found to be increased in PAH patients compared to the controls.

Several aspects need to be kept in mind while interpreting the LDA-based classification model presented here. First, it needs to be emphasized that it was built on a relatively small study with only 80 subjects in total. Thus, it definitely deserves further validation. Furthermore, only metabolites fulfilling certain artificial preselection criteria entered the modeling phase itself; thus, it cannot be ruled out that some variables excluded from further modeling could have theoretically improved model performance, at least to some extent, if they were not excluded. Third, it is also possible that the employment of different modeling approaches might have led to a model with different structures with even improved performance. Lastly, while the eighth-order model was presented in the study as the model with the lowest mean classification error, the overall performances of the best models of the fifth- to ninth-order are quite comparable, as their mean classification errors did not exceed 0.175 (data not shown). The eighth-order model was selected as the best one solely on the basis of the lowest mean classification error criterion. Once the criterion of model dimensionality is additionally considered, it is quite possible that the sixth-order model would be selected as the model of choice, as the reduction of model dimensionality leads to only slight deterioration of the model's mean classification error (0.169) as compared to the eighth-order model (see Table S6 in the Supporting Information).

This study has, admittedly, some limitations worth mentioning. First, the findings presented here require verification in the larger population to confirm clinical relevance. Second, pulmonary hypertensive patients enrolled in this study were under treatment and applied pharmacotherapy, including mainly bosentan, sildenafil, inhaled iloprost, treprostinil, or combined therapy. However, the preliminary impact of applied pharmacotherapy on the metabolic changes observed in this study was evaluated and is provided in Supporting Information (Table S7). Third, besides the fact that mainly patients with PAH (50% with idiopathic one) were included in the study, the mixed etiology remains a crucial problem in clinical practice. Frequently, the pathogenesis of PH can include hallmarks of different clinical groups, which constitutes difficulties in the recognition of dominant etiology and application of proper pharmacotherapy.

5. CONCLUSIONS

This pilot observational study applied untargeted metabolomics and multivariate statistical analyses to evaluate relationships between absolute values of plasma and urine metabolites and clinical parameters, as well as to determine whether metabolomic data could be used to build a classification model allowing for relatively accurate subject classification in the context of PAH. The statistically significant correlations between valine, butyric acid, stearic acid, and 1,2-benzenediol and 6MDW, PA.s, PA.mean, PCWP, and RA.mean, potentially corresponding with the disease severity, were found. Additionally, a panel of eight metabolites, namely pyruvic acid, cholesterol, threonine, 3-(3-hydroxyphenyl)-3-hydroxypropanoic acid, butyric acid, 1,2-benzenediol, glucoheptonic acid, and 2-oxo-glutaric acid, were found to build a relatively accurate LDA-based classification model. The obtained results revealed the great potential of metabolomics for molecular insight into PAH pathobiology and pathophysiology.

https://doi.org/10.1021/acs.jproteome.3c00255
J. Proteome Res. 2024, 23, 2795−2804

The clinical relevance of this study includes the selection of the metabolites' panel specific for PAH. The selected panel of metabolites has potential in early recognition of patients with dyspnea, faster referral to a reference center with full diagnostics, and therefore faster implementation of proper pharmacotherapy. Additionally, RHC parameters are prognostic; however, the test is invasive, so proposed metabolic markers, especially detected in easy available and noninvasive urine samples, could be useful in monitoring disease progression after the implementation of specific PAH pharmacotherapy.

■ ASSOCIATED CONTENT

Data Availability Statement

The data sets analyzed during the current study are available publicly: https://osf.io/as78q/?view_only=26793c1a44c448cdbe2d32c95a83e441

Supporting Information

The Supporting Information is available free of charge at https://pubs.acs.org/doi/10.1021/acs.jproteome.3c00255.

Parameters of analytical methods; figures including urine and plasma metabolic profiles for patients and controls, clustering of patients, controls, and QC samples data for plasma and urine samples, graphical presentations of levels of blood plasma and urine metabolites, values of PC1−PC4 in PAH and control groups, and distribution of mean classification errors; tables including PAH and control metabolite abundances, data distribution of clinical parameters, characteristics of PC1−PC4, components of LDA modeling, and impact of treatment on observed metabolic changes (PDF)

■ AUTHOR INFORMATION

Corresponding Author

Renata Wawrzyniak − *Department of Biopharmaceutics and Pharmacodynamics, Medical University of Gdańsk, 80-416 Gdańsk, Poland;* orcid.org/0000-0002-0763-4589; Email: renata.wawrzyniak@gumed.edu.pl

Authors

Peter Grešner − *Laboratory of Translational Oncology, Intercollegiate Faculty of Biotechnology, University of Gdańsk and Medical University of Gdańsk, 80-211 Gdańsk, Poland*

Ewa Lewicka − *Department of Cardiology and Electrotherapy, Medical University of Gdansk, 80-210 Gdańsk, Poland*

Szymon Macioszek − *Department of Biopharmaceutics and Pharmacodynamics, Medical University of Gdańsk, 80-416 Gdańsk, Poland*

Artur Furga − *Department of General, Endocrine and Transplant Surgery, Invasive Medicine Center, Medical University of Gdańsk, 80-214 Gdańsk, Poland*

Bożena Zieba − *First Department of Cardiology, Medical University of Gdansk, 80-214 Gdańsk, Poland*

Michał J. Markuszewski − *Department of Biopharmaceutics and Pharmacodynamics, Medical University of Gdańsk, 80-416 Gdańsk, Poland*

Alicja Dąbrowska-Kugacka − *Department of Cardiology and Electrotherapy, Medical University of Gdansk, 80-210 Gdańsk, Poland*

Complete contact information is available at: https://pubs.acs.org/10.1021/acs.jproteome.3c00255

Author Contributions

R.W., A.D.-K., and M.J.M. conceived and planned the study and experiments. A.D.-K. and E.L. provided clinical classification of patients. A.F. and B.Z. collected the clinical data of patients. R.W. and S.M. performed the experiments and contributed to sample preparation, analytical measurements, and data processing. P.G. performed all statistical calculations and contributed to the interpretation of the results. R.W. and A.D.-K. took the lead in writing the manuscript. All authors provided critical feedback and helped shape the research, analysis, and manuscript. All authors read and approved the final manuscript.

Notes

The authors declare no competing financial interest.

■ ACKNOWLEDGMENTS

This study was supported by the Medical University of Gdańsk within the "Young Creator of Science" program (grant number 664/529/61/71-1402).

■ ABBREVIATIONS

6MWT, 6 min walk test; ALP, alkaline phosphatase; ALT, alanine aminotransferase; AST, aspartate aminotransferase; BNP, brain natriuretic peptide; CI, cardiac index; CO, cardiac output; CTEPH, chronic thromboembolic pulmonary hypertension patients; DBP, diastolic blood pressure; ECG, electrocardiography; GGT, gamma-glutamyltranspeptidase; HPAH, heritable pulmonary arterial hypertension; HR, heart rate; IPAH, idiopathic pulmonary hypertension; LDA, linear discriminant analysis; mPAP, mean pulmonary artery pressure; mRAP, mean right atrial pressure; OPLS-DA, orthogonal partial least-squares discriminant analysis; PAH, pulmonary arterial hypertension; PCA, principal component analysis; PCWP, pulmonary capillary wedge pressure; PH, pulmonary hypertension; PLT, platelet count; PVR, pulmonary vascular resistance; QC(s), quality control sample(s); RHC, right heart catheterization; SBP, systolic blood pressure; SVR, support vector machine for regression; VIP(s), variable(s) importance in the projection

■ REFERENCES

(1) Kim, D.; George, M. P. Pulmonary Hypertension. *Med. Clin. North Am.* **2019**, *103*, 413−23.

(2) Simonneau, G.; Montani, D.; Celermajer, D. S.; et al. Haemodynamic definitions and updated clinical classification of pulmonary hypertension. *Eur. Respir. J.* **2019**, *53*, 1801913.

(3) Humbert, M.; Kovacs, G.; Hoeper, M. M.; et al. 2022 ESC/ERS Guidelines for the diagnosis and treatment of pulmonary hypertension. *Eur. Heart J.* **2022**, *43*, 3618−731.

(4) Calvo, E.; García-Álvarez, A.; Vázquez, J. The Quest for Metabolic Biomarkers of Pulmonary Hypertension. *J. Am. Coll. Cardiol.* **2016**, *67*, 190−2.

(5) Varghese, M. V.; James, J.; Rafikova, O.; et al. Glucose-6-phosphate dehydrogenase deficiency contributes to metabolic abnormality and pulmonary hypertension. *Am. J. Physiol - Lung Cell Mol. Physiol* **2021**, *320*, L508−21.

(6) Zhao, J. H.; He, Y. Y.; Guo, S. S.; et al. Circulating Plasma Metabolomic Profiles Differentiate Rodent Models of Pulmonary Hypertension and Idiopathic Pulmonary Arterial Hypertension Patients. *Am. J. Hypertens* **2019**, *32*, 1109−17.

(7) Li, M.; Riddle, S.; Zhang, H.; et al. Metabolic Reprogramming Regulates the Proliferative and Inflammatory Phenotype of Adventitial Fibroblasts in Pulmonary Hypertension Through the Transcrip-

tional Corepressor C-Terminal Binding Protein-1. *Circulation* **2016**, *134*, 1105−21.
(8) Cerik, I. B.; Dindas, F.; Koyun, E.; Dereli, S.; Sahin, A.; Turgut, O. O.; Gul, I. New prognostic markers in pulmonary arterial hypertension: CRP to albumin ratio and uric acid. *Clinical Biochemistry* **2022**, *100*, 22−28.
(9) Fiehn, O. Metabolomics - The link between genotypes and phenotypes. *Plant Mol. Biol.* **2002**, *48*, 155−71.
(10) Chen, C.; Luo, F.; Wu, P.; et al. Metabolomics reveals metabolite changes of patients with pulmonary arterial hypertension in China. *J. Cell Mol. Med.* **2020**, *24*, 2484−96.
(11) Harbaum, L.; Rhodes, C. J.; Otero-Núñez, P.; et al. The application of 'omics' to pulmonary arterial hypertension. *Br. J. Pharmacol.* **2021**, *178*, 108−20.
(12) Hemnes, A. R.; Luther, J. M.; Rhodes, C. J.; et al. Human PAH is characterized by a pattern of lipid-related insulin resistance. *JCI Insight* **2019**, *4*, 4.
(13) Rhodes, C. J.; Ghataorhe, P.; Wharton, J.; et al. Plasma Metabolomics Implicates Modified Transfer RNAs and Altered Bioenergetics in the Outcomes of Pulmonary Arterial Hypertension. *Circulation* **2017**, *135*, 460−75.
(14) Zhao, Y.; Peng, J.; Lu, C.; et al. Metabolomic heterogeneity of pulmonary arterial hypertension. *PLoS One* **2014**, *9*, No. e88727.
(15) Maniscalco, M.; Fuschillo, S.; Paris, D.; Cutignano, A.; Sanduzzi, A.; Motta, A. Chapter Five-Clinical metabolomics of exhaled breath condensate in chronic respiratory diseases. *Adv. Clinical Chem.* **2019**, *88*, 121−149.
(16) Struck-Lewicka, W.; Wawrzyniak, R.; Artymowicz, M.; et al. GC-MS-based untargeted metabolomics of plasma and urine to evaluate metabolic changes in prostate cancer. *J. Breath Res.* **2020**, *14*, 047103.
(17) Struck-Lewicka, W.; Kordalewska, M.; Bujak, R.; et al. Urine metabolic fingerprinting using LC-MS and GC-MS reveals metabolite changes in prostate cancer: A pilot study. *J. Pharm. Biomed Anal* **2015**, *111*, 351−61.
(18) Dunn, W. B.; Broadhurst, D.; Begley, P.; et al. Procedures for large-scale metabolic profiling of serum and plasma using gas chromatography and liquid chromatography coupled to mass spectrometry. *Nat. Protoc* **2011**, *6*, 1060−83.
(19) Harris, R. A.; Joshi, M.; Jeoung, N. H. Mechanisms responsible for regulation of branched-chain amino acid catabolism. *Biochem. Biophys. Res. Commun.* **2004**, *313*, 391−396.
(20) Cojocaru, E.; Magdalena Leon-Constantin, M.; Ungureanu, C.; et al. Hypolipemiant Actions and Possible Cardioprotective Effects of Valine and Leucine: An Experimental Study. *Medicina (B Aires)* **2021**, *57*, 239.
(21) Noguchi, Y.; Zhang, Q.-W.; Sugimoto, T.; et al. Network analysis of plasma and tissue amino acids and the generation of an amino index for potential diagnostic use. *Am. J. Clin. Nutr.* **2006**, *83*, 513S−519S.
(22) Sampath, H.; Ntambi, J. M. The fate and intermediary metabolism of stearic acid. *Lipids* **2005**, *40*, 1187−91.
(23) Kim, H. S.; Yoo, H. J.; Lee, K. M.; et al. Stearic acid attenuates profibrotic signalling in idiopathic pulmonary fibrosis. *Respirology* **2021**, *26*, 255−63.
(24) Ríos-Covián, D.; Ruas-Madiedo, P.; Margolles, A.; et al. Intestinal Short Chain Fatty Acids and their Link with Diet and Human Health. *Front Microbiol* **2016**, *7*, 185.
(25) Wong, J. M. W.; De Souza, R.; Kendall, C. W. C.; et al. Colonic health: Fermentation and short chain fatty acids. *Journal of Clinical Gastroenterology* **2006**, *40*, 235−43.
(26) Vinolo, M. A. R.; Rodrigues, H. G.; Nachbar, R. T.; et al. Regulation of Inflammation by Short Chain Fatty Acids. *Nutrients* **2011**, *3*, 858−76.
(27) Hong, F.; Pan, S.; Guo, Y.; et al. PPARs as Nuclear Receptors for Nutrient and Energy Metabolism. *Molecules* **2019**, *24*, 2545.
(28) Onyszkiewicz, M.; Gawrys-Kopczynska, M.; Konopelski, P.; et al. Butyric acid, a gut bacteria metabolite, lowers arterial blood pressure via colon-vagus nerve signaling and GPR41/43 receptors. *Pflügers Arch - Eur. J. Physiol* **2019**, *471*, 1441−53.
(29) Heaney, L. M. Applying mass spectrometry-based assays to explore gut microbial metabolism and associations with disease. *Clinical Chemistry and Laboratory Medicine (CCLM)* **2020**, *58*, 719−732.
(30) Thenappan, T.; Khoruts, A.; Chen, Y.; et al. Can intestinal microbiota and circulating microbial products contribute to pulmonary arterial hypertension? *Am. J. Physiol Circ Physiol* **2019**, *317*, H1093−101.
(31) Mansoor, S.; Gupta, N.; Luczy-Bachman, G.; et al. Protective effects of memantine and epicatechin on catechol-induced toxicity on Müller cells in vitro. *Toxicology* **2010**, *271*, 107−14.
(32) Bukowska, B.; Michałowicz, J.; Marczak, A. The effect of catechol on human peripheral blood mononuclear cells (in vitro study). *Environ. Toxicol Pharmacol* **2015**, *39*, 187−93.
(33) Jordan, J.; Lipp, A.; Tank, J.; et al. Catechol-O-Methyltransferase and Blood Pressure in Humans. *Circulation* **2002**, *106*, 460−5.
(34) Xu, W.; Janocha, A. J.; Erzurum, S. C. Metabolism in Pulmonary Hypertension. *Annu. Rev. Physiol.* **2021**, *83*, 551−76.
(35) Xu, W.; Erzurum, S. C. Endothelial Cell Energy Metabolism, Proliferation, and Apoptosis in Pulmonary Hypertension. *Compr. Physiol.* **2010**, 357−372.
(36) Xu, W.; Koeck, T.; Lara, A. R.; et al. Alterations of cellular bioenergetics in pulmonary artery endothelial cells. *Proc. Natl. Acad. Sci. U. S. A.* **2007**, *104*, 1342−7.
(37) Lundgrin, E. L.; Park, M. M.; Sharp, J.; et al. Fasting 2-Deoxy-2-[18 F]fluoro- d -glucose Positron Emission Tomography to Detect Metabolic Changes in Pulmonary Arterial Hypertension Hearts over 1 Year. *Ann. Am. Thorac Soc.* **2013**, *10*, 1−9.
(38) Neveu, J.; Cano, A.; Hoebeke, C.; Acquaviva-Bourdain, C.; Gastaldi, M.; Chabrol, B. Hyperglycinemia in a 5-Week-Old Boy with Pulmonary Arterial Hypertension. *Clinical Chemistry* **2022**, *68*, 604−606.
(39) Fijalkowska, I.; Xu, W.; Comhair, S. A. A.; et al. Hypoxia Inducible-Factor1α Regulates the Metabolic Shift of Pulmonary Hypertensive Endothelial Cells. *Am. J. Pathol.* **2010**, *176*, 1130−8.
(40) Stephens, O. R.; Weiss, K.; Frimel, M.; et al. Interdependence of hypoxia and β-adrenergic receptor signaling in pulmonary arterial hypertension. *Am. J. Physiol Cell Mol. Physiol* **2019**, *317*, L369−80.
(41) Wu, N.; Yang, M.; Gaur, U.; et al. Alpha-Ketoglutarate: Physiological Functions and Applications. *Biomol Ther (Seoul)* **2016**, *24*, 1−8.
(42) MacMahon, S.; Duffy, S.; Rodgers, A.; et al. Blood cholesterol and vascular mortality by age, sex, and blood pressure: a meta-analysis of individual data from 61 prospective studies with 55 000 vascular deaths. *Lancet* **2007**, *370*, 1829−1839.
(43) Kopeć, G.; Waligóra, M.; Tyrka, A.; et al. Low-density lipoprotein cholesterol and survival in pulmonary arterial hypertension. *Sci. Rep* **2017**, *7*, 41650.
(44) Jonas, K.; Waligóra, M.; Magoń, W.; et al. Prognostic role of traditional cardiovascular risk factors in patients with idiopathic pulmonary arterial hypertension. *Arch Med. Sci.* **2019**, *15*, 1397−406.
(45) Parlak, E. S.; Alisik, M.; Karalezli, A.; et al. Are the thiol/disulfide redox status and HDL cholesterol levels associated with pulmonary embolism?: Thiol/disulfide redox status in pulmonary embolism. *Clinical Biochemistry* **2017**, *50*, 1020−1024.

https://doi.org/10.1021/acs.jproteome.3c00255
J. Proteome Res. 2024, 23, 2795−2804